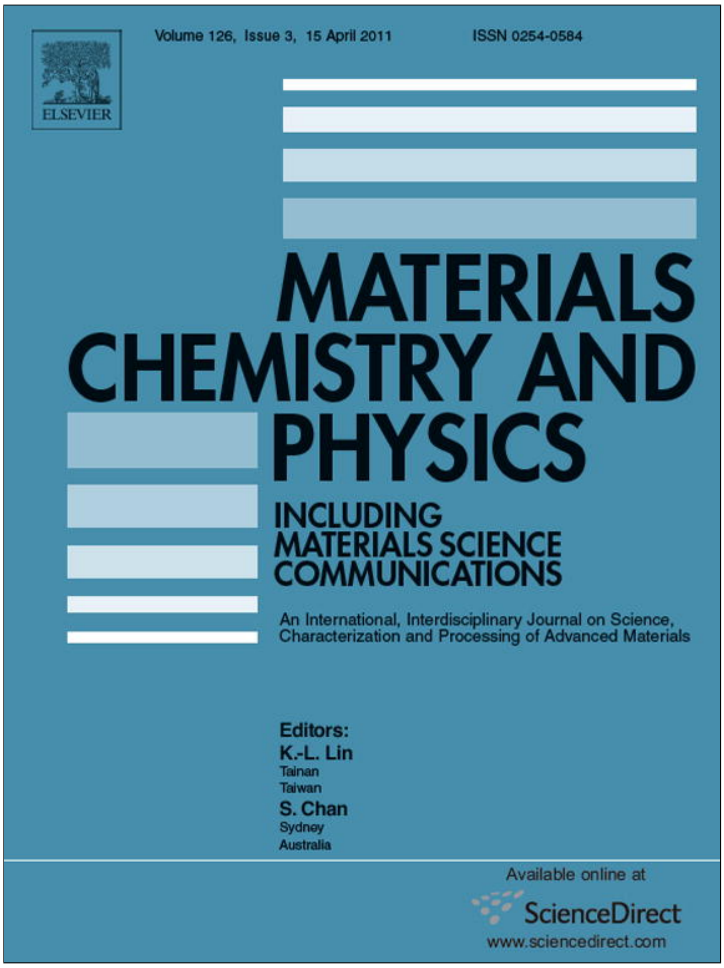

Volume 126, Issue 3, 15 April 2011 ISSN 0254-0584

MATERIALS CHEMISTRY AND PHYSICS

INCLUDING MATERIALS SCIENCE COMMUNICATIONS

An International, Interdisciplinary Journal on Science, Characterization and Processing of Advanced Materials

Materials Chemistry and Physics 126 (2011) 873–879

Contents lists available at ScienceDirect

Materials Chemistry and Physics

journal homepage: www.elsevier.com/locate/matchemphys

Inhibitive effect of synthesized 2-(3-pyridyl)-3,4-dihydro-4-quinazolinone as a corrosion inhibitor for mild steel in hydrochloric acid

N.S. Ayati [a], S. Khandandel [a], M. Momeni [a,*], M.H. Moayed [a], A. Davoodi [b], M. Rahimizadeh [c]

[a] Metallurgical and Materials Engineering Department, Faculty of Engineering, Ferdowsi University of Mashhad, Azadi Square, Mashhad 91775-1111, Iran
[b] Materials Engineering Department, Sabzevar Tarbiat Moallem University, Sabzevar 391, Iran
[c] Chemistry Department, Faculty of Science, Ferdowsi University of Mashhad, Mashhad 91775-1111, Iran

ARTICLE INFO

Article history:
Received 14 June 2010
Received in revised form 8 December 2010
Accepted 9 December 2010

Keywords:
Corrosion
Adsorption
Surface
Organic compounds

ABSTRACT

In this study, the inhibitive effect of synthesized 2-(3-pyridyl)-3,4-dihydro-4-quinazolinone (PDQ) as a new corrosion inhibitor for mild steel in 0.1 M hydrochloric acid media is investigated employing potentiodynamic polarization, electrochemical impedance spectroscopy (EIS) and linear polarization resistance (LPR) techniques. The results show PDQ reduces anodic dissolution, retards the hydrogen evolution reaction and its adsorption obeys the Langmuir's adsorption isotherm. By increase in temperature, corrosion current density increases, however, its increase is lower in the presence of PDQ. By increase in temperature from 25 °C to 45 °C the inhibition efficiency decreases from 93% to 83% in solution containing 200 ppm inhibitor. Thermodynamic adsorption parameters show that PDQ is absorbed by a spontaneous exothermic process and its adsorption mechanism is combination of physical and chemical style.

1. Introduction

Mild steel is widely applied as constructional material in many industries due to its excellent mechanical properties and low cost. Some of the important fields of applications of mild steel are acid pickling in sulfuric acid (H_2SO_4) and hydrochloric acid (HCl), industrial cleaning, acid descaling, oil-well acidizing and petrochemical processes, however the main problem of applying mild steel is its dissolution in acidic solutions. Several methods are available for corrosion prevention. Employing inhibitors is one of the cost-effective protection methods of metals and alloys in acids such as hydrochloric acid [1–5]. Generally, Inhibitors are organic components which have nitrogen, oxygen and sulfur in their molecular structure [1–12]. It has been reported that heterocyclic organic components have better inhibition role in acidic media [5–10]. The inhibiting effect is generally explained by the formation of a physical and/or chemical adsorption film barrier on the metal surface [7,13]. Physisorption involves electrostatic forces between ionic charges or dipoles on the adsorbed species and the electric charge at metal/solution interface. Chemisorption, involves charge sharing or charge transfer from the inhibitor molecules to the metal surface to form a coordinate type bond. In fact, electron transfer is normally proposed for transition metals having vacant low-energy electron orbital. Chemisorption is characterized by stronger adsorption energy than physical adsorption. The inhibition efficiency for Physisorption is higher at lower temperatures while Chemisorption is more stable at higher temperatures. Organic molecules could be adsorbed on the metal surface by (a) electrostatic interaction between charged surface of metal and the charge of the inhibitor, (b) interaction of unshared electron pairs in the inhibitor molecule with the metal, (c) interaction of p-electron with metal and (d) a combination of the (a–c) types [14,15]. It has been reported that the pyridyl derivatives act as an inhibitor for various alloys in different acidic media [16–20]. This family of organic compounds has nitrogen in their molecular structure and also heterocyclic group which can create the inhibition properties in acidic media and can be adsorbed onto the surface.

The objective of this study was to investigate a newly synthesized pyridyl derivative namely of 2-(3-pyridyl)-3,4-dihydro-4-quinazolinone as a new corrosion inhibitor for mild steel in 0.1 M HCl media.

2. Materials and methods

Fig. 1 shows molecular structure of the pyridyl derivative used in this study named as 2-(3-pyridyl)-3,4-dihydro-4-quinazolinone (PDQ) (or 2-phenylquinazolin-4(3H)-one). The titled compound was synthesized from the reaction of equimolar *ortho*-aminobezamide with 3-pyridylaldehyde (or benzaldehyde) in the presence of 0.1 M aqueous solution of iodine/potassium iodide at room temperature. The obtained compound melting temperature is 289–292 °C [21]. For corrosion test the electrolyte solution was 0.1 M HCl which produces pH = 1 (acidic pH in which the iron oxides are not stable and applicable for acid pickling process) and three inhibitor concentrations of 50, 100 and 200 ppm were chosen. The reference electrode and auxiliary electrode were saturated calomel electrode (SCE) and a

---

[*] Corresponding author. Tel.: +98 5118763305; fax: +98 5118763301.
E-mail addresses: mojtaba.momeni@stu-mail.um.ac.ir, mojtaba.momeni@gmail.com (M. Momeni).

0254-0584/$ – see front matter © 2010 Elsevier B.V. All rights reserved.
doi:10.1016/j.matchemphys.2010.12.023

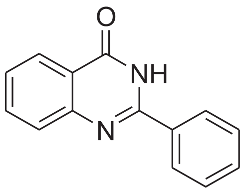

Fig. 1. Molecular structure of 2-(3-pyridyl)-3,4-dihydro-4-quinazolinone (PDQ).

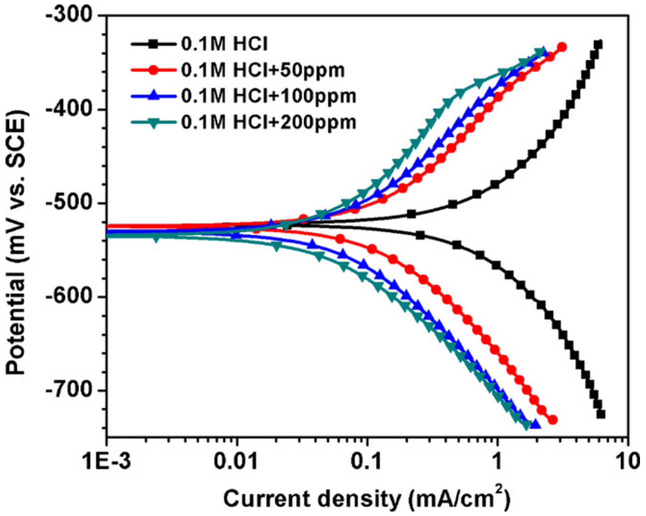

Fig. 2. Polarization diagram in different inhibitor concentration.

2 cm^2 foil of platinum, respectively. Working electrode was mild steel and its chemical composition was as follows (wt%): 0.16% C, 0.1% Si, 0.4% Mn, 0.02% S, 0.13% P, and Fe balance. Potentiodynamic polarization was conducted at constant sweep rate of 1 mV s^{-1} and scanning range of −200 to +200 mV around the open circuit potential (OCP). Before each experiment, the working electrode was immersed for 60 min in the test cell [22] until corrosion potential reaches a steady state condition. All tests were carried out at constant temperature (within ±2 °C) by controlling the cell temperature using a water bath. EIS measurements were performed in frequency range of 10 kHz to 10 mHz with amplitude of 15 mV peak-to-peak using AC signals at open circuit potential. Liner polarization resistance (LPR) was also done by specimen polarization in different inhibitor concentrations from −15 mV to +15 mV around corrosion potential by 10 mV min^{-1} scan rate. The LPR value was measured by calculating the slope of current–potential plot at corrosion potential. Electrochemical tests were conducted by means of ACM Instruments automated potentiostat (Gill AC).

The molecular structures of the PDQ has been geometrically optimized by DFT method using B3LYP level and 3–21G** basis set with Gaussian 98. Quantum chemical parameters such as the highest occupied molecular orbital (HOMO), the lowest unoccupied molecular orbital (LUMO), energy gap ($\Delta E = E_{HOMO} - E_{LUMO}$), and dipole moment ($\mu$) have calculated.

3. Results and discussion

3.1. Tafel polarization

Cathodic and anodic polarization plots of mild steel with different concentrations of PDQ in 0.1 M HCl at 25 °C are shown in Fig. 2. Electrochemical parameters include corrosion potential (E_{corr}), corrosion current density (i_{corr}), and cathodic and anodic Tafel slopes (β_c and β_a) were measured by Tafel extrapolating of the anodic and cathodic lines and listed in Table 1. The degree of surface coverage (θ) and the percentage of inhibition efficiency (%η) were calculated using the following equations [3,10,23]:

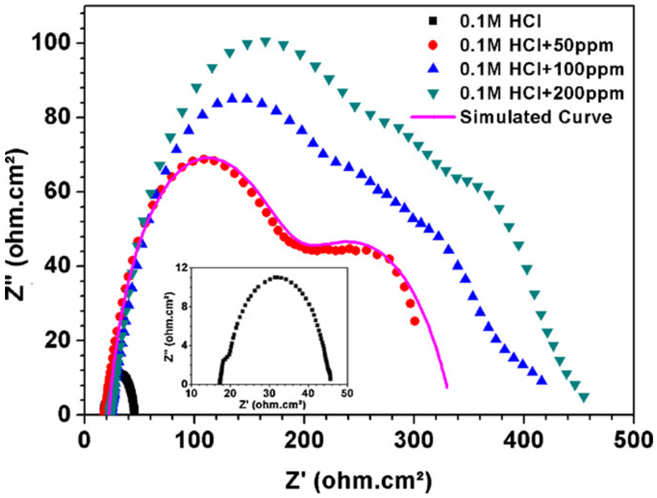

Fig. 3. Nyquist plot for PDQ in different concentration. Inserted micrograph represents the Nyquist plot in uninhibited solution.

$$\theta = \frac{i^0_{corr} - i_{corr}}{i^0_{corr}} \tag{1}$$

$$\%\eta = \theta \times 100 \tag{2}$$

where i^0_{corr} and i_{corr} are corrosion current densities of mild steel in the absence and presence of inhibitor, respectively. From the results in Table 1, it can be seen that the values of corrosion current density (i_{corr}) in the presence of inhibitor is significantly lower than uninhibited solution. Fig. 2 shows a slight decrease in anodic and cathodic Tafel slopes for inhibited solution in all concentrations. Although in all concentrations, PDQ is adsorbed on metal surface, no important change in Tafel slop was observed. Therefore, the inhibition role of this compound is not due to the interference on the reactions of metal dissolution and reduction of hydrogen ion [24]; PDQ acts as adsorptive inhibitor, i.e., it reduces anodic dissolution and retard the hydrogen evolution reaction via blocking the active reaction sites on the metal surface.

3.2. Electrochemical impedance spectroscopy (EIS)

The result of the EIS measurement was figured by Nyquist plots (see Fig. 3). In this study, Nyquist plots of solutions containing inhibitor show two capacitive loops, whereas the impedance spectra in absence of inhibitor present only one capacitive loop. In this case, the capacitive loop at higher frequencies arises from charge transfer double layer and the second loop at low frequency can be attributed to the adsorption of inhibitor on the metal surface. The replacement of double layer and inhibitor layer is reported in some studies [25–27]. This fact can be proved by changing temperature from 25 °C to 45 °C as shown in Fig. 4. By increasing temperature, second time constant was removed. Consequently, the second time

Table 1
Calculated potentiodynamic polarization parameters for different concentrations of PDQ.

C (ppm)	E_{corr} (mV vs. SCE)	i_{corr} (μA cm^{-2})	β_c (mV decade^{-1})	β_a (mV decade^{-1})	θ	%η
Blank	−522	750 ± 2	183	180	–	–
50	−525	74 ± 0.2	125	141	0.90	90.13
100	−529	62 ± 0.2	124	144	0.92	91.73
200	−534	53 ± 0.2	132	155	0.93	92.93

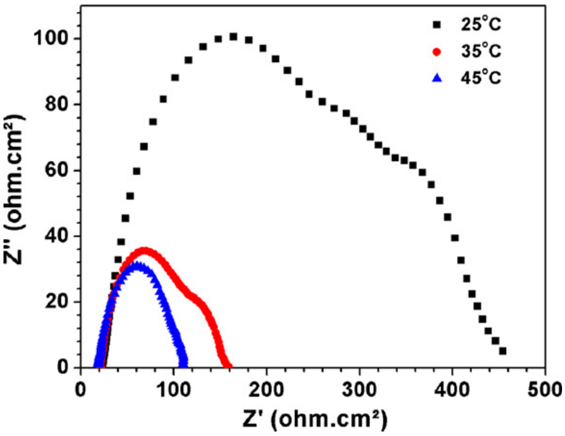

Fig. 4. Effect of temperature on Nyquist plots of 200 ppm PDQ.

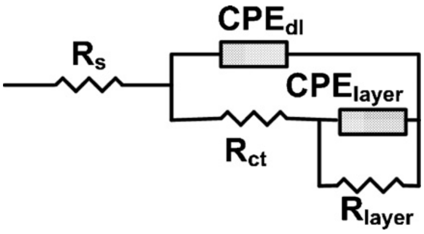

Fig. 5. Equivalent circuit which used to fit the EIS data of mild steel in different inhibitor concentration.

constant arises from a formed inhibitor layer on surface, so by reducing the temperature this formed layer is thickened.

Equivalent circuit that is used to fit the EIS data of mild steel is shown in Fig. 5. According to the equivalent circuits the solution resistance (R_s), the charge transfer resistance (R_{ct}), the constant phase element (CPE) parameters and formed inhibitor layer related parameters were extracted and listed in Table 2. The R_{ct} values increased with increase in inhibitor concentration. This indicates formation of an insulated adsorption layer [14]. Inhibitor efficiency can also be estimated by charge transfer resistance according to the following equation [28]:

$$\%\eta = \frac{R - R^0}{R} \times 100 \tag{3}$$

where R^0 and R are charge transfer resistances of mild steel in the absence and presence of inhibitor, respectively. Table 2 lists efficiency values, which are in close correlation with those of polarization results. Both polarization and EIS results show that efficiency increases with increasing the inhibitor concentration.

In order to accurate study of impedance behavior of these two electric double layers, CPE was used as the alternate for capacitor. The impedance of the CPE is presented as [29]:

$$Z_{CPE} = \frac{1}{P(i\omega)^n} \tag{4}$$

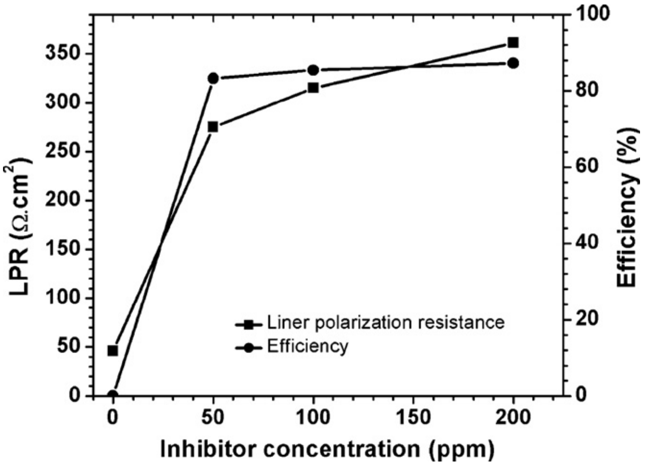

Fig. 6. Liner polarization resistance (LPR) results for PDQ in different inhibitor concentrations.

where P is the magnitude of the CPE, ω the angular frequency, and n as the deviation parameter. For a circuit including a CPE$_{dl}$, the double layer capacitance (C_{dl}) can be calculated from CPE parameter values P and n using the expression [30]:

$$C_{dl} = \frac{P\omega_{max}^{n-1}}{\sin(n(\pi/2))} \tag{5}$$

In the Helmholtz model of the surface adsorbed film capacitance, it is defined that the capacitance is inversely proportional to the surface film thickness [31].

$$C_{dl} = \frac{\varepsilon^0 \varepsilon}{d} S \tag{6}$$

where d is the thickness of the film, S is the surface of the electrode, ε^0 is the permittivity of the air, and ε is the local dielectric constant. The decrease in C_{dl} by increasing inhibitor concentration to 200 ppm is due to the steady replacement of water molecules by the adsorptive inhibitor molecules at metal/solution interface, which is leading to a protective film on the steel surface and increasing the d value.

3.3. Liner polarization resistance (LPR)

Another useful and fast method for inhibitors study is LPR method. Fig. 6 shows the linear polarization resistance (LPR) and resulted efficiency calculated according to the Eq. (3) for PDQ in different inhibitor concentrations at 25 °C. It shows that by increasing the inhibitor concentration, LPR value increases. Based on the Eq. (7), by increase in LPR value, corrosion current density decreases.

$$i_{corr} = \frac{\beta_a \beta_c}{2.3\mathrm{LPR}(\beta_a + \beta_c)} \tag{7}$$

Regarding to the Eq. (7), the values of i_{corr} for inhibited solutions are lower than those of uninhibited solutions. The values of efficiency of PDQ in all concentrations show that by increasing the inhibitor concentration the efficiency increases.

Table 2
Calculated EIS parameters from equivalent circuit for different concentrations of PDQS.

C (ppm)	R_s (Ω cm^2)	R_{ct} (Ω cm^2)	CPE$_{dl}$		R_{layer} (Ω cm^2)	CPE$_{layr}$		C_{dl} (μF cm^{-2})	θ	%η
			P (μF cm^{-2})	n		P (F cm^{-2})	n			
Blank	17.63	23.13	504.94	0.83	–	–	–	200.346	–	–
50	22.17	164.78	222.07	0.86	148.39	0.0098	0.62	119.267	0.88	88
100	24.50	215.00	221.00	0.85	165.12	0.0070	0.60	117.537	0.91	91
200	23.60	254.43	216.16	0.80	187.49	0.0065	0.60	116.224	0.92	92

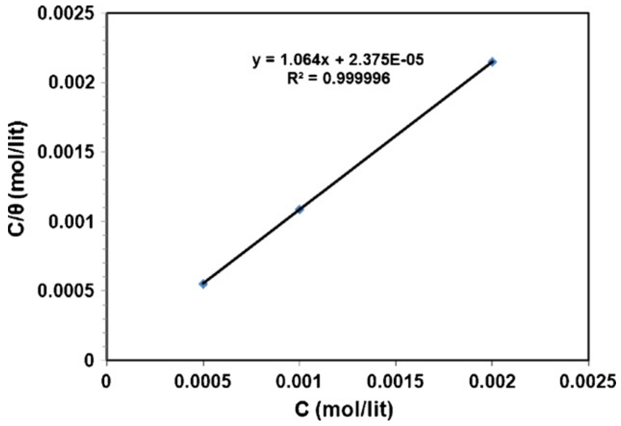

Fig. 7. Langmuir adsorption isotherm of inhibitors in 0.1 M HCl at 25 °C.

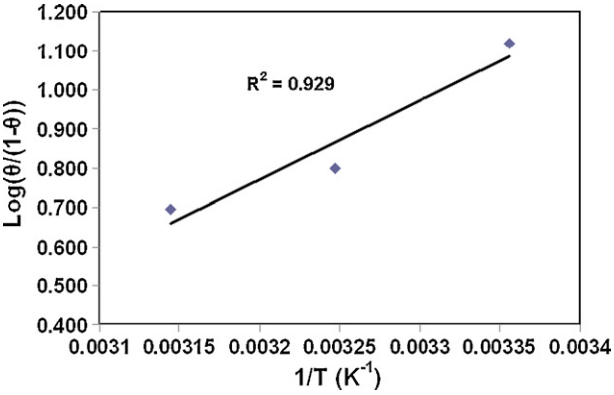

Fig. 8. $\log(\theta/1-\theta)$ vs. $1/T$ for adsorption of PDQ

3.4. Adsorption isotherm

Invaluable information of interaction between adsorptive inhibitor molecules and metal surface can be provided by adsorption isotherm investigation [32,33]. The adsorption of organic compounds can be expressed by two main types of interactions: physical adsorption and chemical adsorption. There are some factors that influence the adsorption processes including the nature and charge of metal, the chemical of inhibitor, and the type of electrolyte [24]. Adsorption of organic molecule at the metal\solution interface can be elucidated by substitution adsorption process between the organic molecules in aqueous solution and water molecule on metal surface [14].

$$\mathrm{Org}_{(sol)} + x\mathrm{H_2O}_{(ads)} \rightarrow \mathrm{Org}_{(ads)} + x\mathrm{H_2O}_{(sol)} \tag{8}$$

where $\mathrm{Org}_{(sol)}$ and $\mathrm{Org}_{(ads)}$ are inhibitor molecules dissolved in solution and adsorbed on metal surface respectively. $\mathrm{H_2O}_{(ads)}$ is water molecule on metal surface, $\mathrm{H_2O}_{(sol)}$ is water molecule in solution, and x is size ratio and represents the number of molecules of water replaced by inhibitor molecules. For inhibitor studies, it is found that the data from electrochemical test can be fitted by Langmuir model. According to this model, the surface coverage (θ) is proportional to inhibitor concentration (C) [10,32].

$$\frac{\theta}{1-\theta} = K_{ads}C \tag{9}$$

By rearranging Eq. (9):

$$\frac{C}{\theta} = \frac{1}{K_{ads}} + C \tag{10}$$

where K_{ads} is equilibrium constant for adsorption reaction. This is a general model and has been used for inhibitor studies [14,32–35]. Fig. 7 shows the C/θ vs. C. The strong correlation ($R^2 = 0.999996$) demonstrates that adsorption of this inhibitor on mild steel follow this isotherm and supposed that the adsorbed molecules occupy only one site and there are no interactions with other adsorbed species [33]. According to Eq. (10), K_{ads} can be calculated from intercept line on C/θ axis. With the following equation, $\Delta G_{ads}{}^{\circ}$ can be calculated from K_{ads} [33–35]:

$$\Delta G^{\circ}_{ads} = -RT\ln(55.5K_{ads}) \tag{11}$$

where R is gas constant and T is absolute temperature of experiment and the constant value of 55.5 is the concentration of water in solution in mol dm^{-3} [24]. By using the Eq. (11), the calculated $\Delta G_{ads}{}^{\circ}$ will be −36.332 kJ mol^{-1}. The negative sign of $\Delta G_{ads}{}^{\circ}$ demonstrates that the inhibitor is spontaneously adsorbed onto the metal surface [6,33]. Normally, the magnitude of $\Delta G_{ads}{}^{\circ}$ around −20 kJ mol^{-1} or less negative is assumed for electrostatic interactions exist between inhibitor and the charged metal surface (i.e., physisorption). Those around −40 kJ mol^{-1} or more negative are indication of charge sharing or transferring from organic species to the metal surface to form a coordinate type of metal bond (i.e., chemisorption) [9,10,32,34]. Some authors have reported the values of $\Delta G_{ads}{}^{\circ}$ less negative than −40 kJ mol^{-1} for physical adsorption frequently interpreted as the formation of an adsorptive film with an electrostatic character [26,33].

The heat of adsorption process (Q_{ads}) can also be estimated from the variation of surface coverage vs. reciprocal of temperature by using the Langmuir's adsorption isotherm as following [33,36–38]

$$\log\left(\frac{\theta}{1-\theta}\right) = \log(A) + \log(C) - \frac{Q_{ads}}{2.303RT} \tag{12}$$

where A is a constant and Q_{ads} is the heat of adsorption which is almost equal to enthalpy of adsorption process ($\Delta H_{ads}{}^{\circ}$) [24]. Fig. 8 represents the variation of $\log(\theta/1-\theta)$ vs. $1/T$ for PDQ. The heat of adsorption can be obtained from the slope of the line, which is equal to ($-Q_{ads}/2.303R$). The entropy of adsorption process ($\Delta S_{ads}{}^{\circ}$) can also be calculated based on the following thermodynamic basic equation [10,32,33]:

$$\Delta G^{\circ}_{ads} = \Delta H^{\circ}_{ads} - T\,\Delta S^{\circ}_{ads} \tag{13}$$

$\Delta H_{ads}{}^{\circ}$ and $\Delta S_{ads}{}^{\circ}$ values are given in −38.595 kJ mol^{-1} and 0.251 kJ mol^{-1} respectively. Valuable information about the mechanism of corrosion inhibition can be provided by the values of thermodynamic parameters for the adsorption of inhibitor. An

Table 3
Potentiodynamic polarization results in the presence and absence of 200 ppm PDQ at different temperatures.

C (ppm)	Temperature (°C)	E_{corr} (mV vs. SCE)	i_{corr} (μA cm^{-2})	β_c (mV decade^{-1})	β_a (mV decade^{-1})	θ	%η
Blank	25	−522	750 ± 2	183	180	–	–
	35	−524	1219 ± 5	190	174	–	–
	45	−525	1860 ± 5	188	169	–	–
200	25	−534	53 ± 0.2	132	155	0.93	92.93
	35	−508	166 ± 0.4	161	136	0.86	86.38
	45	−530	312 ± 0.5	154	142	0.83	83.23

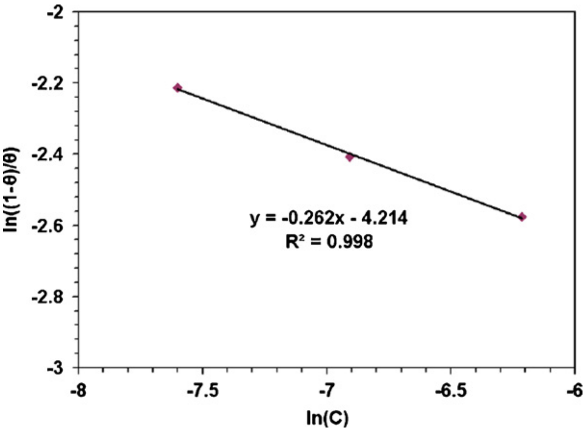

Fig. 9. log(1 − θ/θ) vs. 1/C for adsorption of PDQ.

endothermic adsorption process ($\Delta H_{ads}{}^\circ > 0$) is due to chemisorption while an exothermic adsorption process ($\Delta H_{ads}{}^\circ > 0$) may be attributed to physisorption, chemisorption or a mixture of both [10,30]. When the process of adsorption is exothermic, physisorption can be distinguished from chemisorptions according to the absolute value of $\Delta H_{ads}{}^\circ$. For physisorption processes, this magnitude is usually lower than 40 kJ mol^{-1} while its value is around 100 kJ mol^{-1} for chemisorptions [15]. In this work, the negative sign of $\Delta H_{ads}{}^\circ$ indicated that the adsorption of inhibitors used is exothermic. Base on the results of the present work, the calculated $\Delta G_{ads}{}^\circ$ and $\Delta H_{ads}{}^\circ$ values for PDQ show that adsorption mechanism is not completely physical or chemical and a combination of physisorption and chemisorption exists between the inhibitors and metal surface [32]. The positive sign of $\Delta S_{ads}{}^\circ$ arise from substitutional process, which can be attributed to the increase in the solvent entropy and more positive water desorption entropy [26,39]. It also interpreted with increase of disorders due to the more water molecules which can be desorbed from the metal surface by one inhibitor molecule [26,33].

It was reported elsewhere [40] that the value of $\Delta G_{ads}{}^\circ$ can also be calculated according to the following formula:

$$\ln\left(\frac{1-\theta}{\theta}\right) = \frac{\Delta G^\circ_{ads}}{\phi} - \frac{RT\ln C}{\phi} \tag{14}$$

In which φ is a constant value arise from statistical physics approach. By this method $\Delta G_{ads}{}^\circ$ can by calculated directly in each temperature. Fig. 9 shows the results of ln((1 − θ)/θ) vs. lnC at 25 °C. Φ and $\Delta G_{ads}{}^\circ$ can be calculated and the value of −39.85 kJ mol^{-1} can be obtained by using the slope and the ordinate axis intercept of the straight line. This value of $\Delta G_{ads}{}^\circ$ shows close correlation with last approach.

3.5. Effect of temperature

The adsorption phenomenon has been successfully explained by thermodynamic parameter. To elucidate the inhibition properties of inhibitor, the kinetic model was another useful tool to explain the mechanism of corrosion inhibition for the inhibitor. Since many changes on the metal surface such as rapid etching and desorption of inhibitor occurs and also the inhibitor itself may undergo decomposition, effect of temperature on the inhibited acid–metal reaction is very complicated [10]. The change of the corrosion rate with the temperature was studied in the absence and presence of PDQ in 0.1 M HCl. For this purpose, polarization readings were performed at different temperatures from 25 °C to 45 °C in absence and presence of 200 ppm of PDQ (Fig. 10). It is obvious that the values of i_{corr} increases by increasing in temperature in both solutions and the efficiency value changes and decreases from 93% to 83%. Fig. 10 shows that raising the temperature has no significant effect on the corrosion potentials; but leads to a higher corrosion rate (i_{corr}). The extracted results of potentiodynamic curves are shown in Table 3. The activation parameters for the corrosion process can

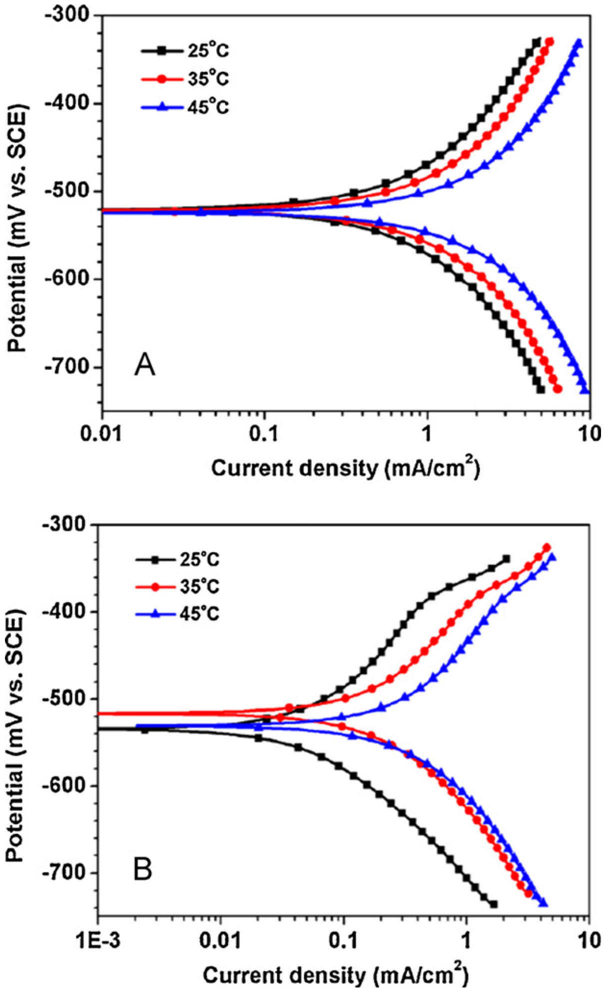

Fig. 10. Anodic and cathodic curves for mild steel in different temperatures (a) bulk solution and (b) in the presence of 200 ppm PDQ.

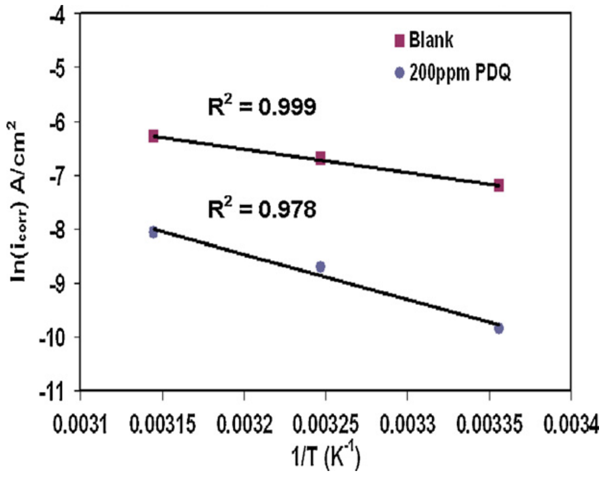

Fig. 11. ln(i_{corr}) vs. 1/T for mild steel in 0.1 M HCl in the absence and presence 200 ppm PDQ.

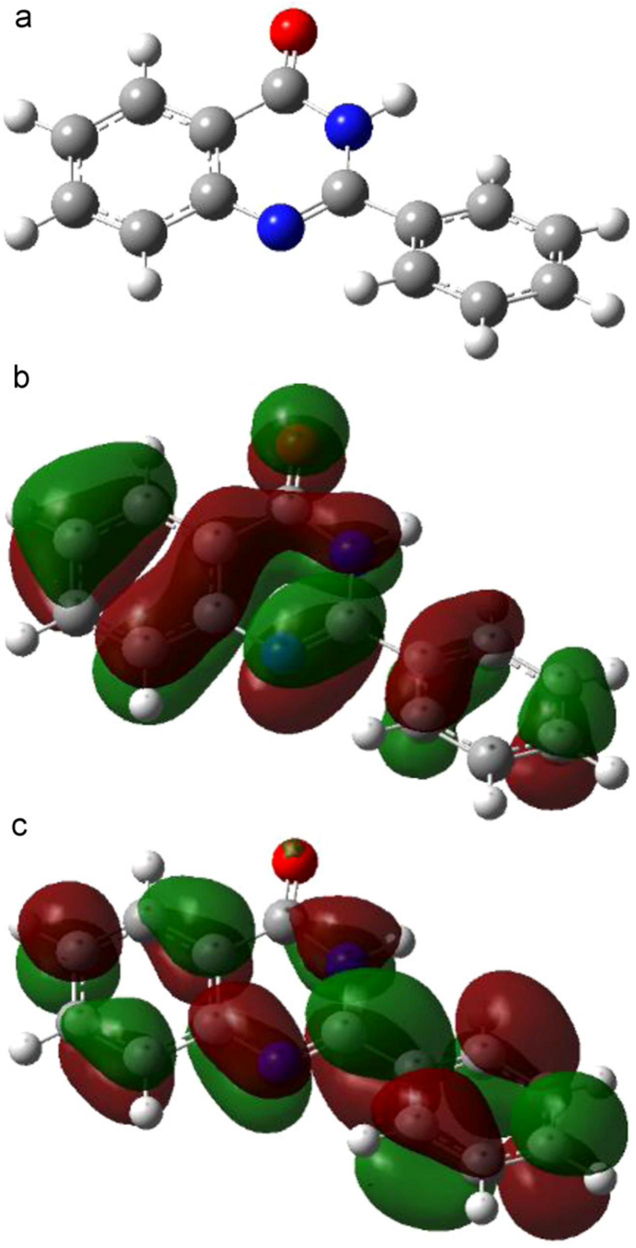

Fig. 12. (a) Molecular structure, (b) HOMO and (c) LUMO of PDQ.

be calculated from Arrhenius equation:

$$\ln(i_{\text{corr}}) = \ln A - \frac{E_a}{RT} \tag{15}$$

where E_a represents the apparent activation energy, R the gas constant, A the pre-exponential factor and i_{corr} is the corrosion rate, obtained from the polarization method. Arrhenius plots for the corrosion rate of mild steel were given in Fig. 11. Values of E_a for mild steel in 0.1 M HCl with 200 ppm of PDQ and in the absence of inhibitor were estimated by calculating the slop of $\ln(i_{\text{corr}})$ vs. $1/T$. These results show that by adding 200 ppm of PDQ to the solution containing 0.1 M HCl, the activation energy for corrosion process increases from 35.8 kJ mol^{-1} to 65.856 kJ mol^{-1}. The increase in the corrosion current density activation energy indicates that dissolution of mild steel in 0.1 M HCl in the presence of inhibitor is lower than the solution with no inhibitor. It has been reported that higher E_a in presence of inhibitors for mild steel in comparison with blank solution is typically showing physisorption [32]. Considering E_a values, PDQ has an electrostatic interaction on metal surface (physisorption).

3.6. *Quantum chemical study*

To investigate the correlation between molecular structure of PDQ and its inhibition effect, quantum chemical study has been performed. Geometric structures and electronic properties of PDQ has been calculated by DFT method using B3LYP level and $3–21G^{**}$ basis set. Fig. 12 shows optimized molecular structures, HOMO and LUMO of PDQ. It shows that the benzene ring, O and N atoms have larger electric density. It is suggested that the benzene ring, O and N atoms can be suitable places for adsorption onto surface, especially in case of O and N because of their lone pair of electrons. PDQ molecules can be directly adsorbed at the steel surface on the basis of donor–acceptor interactions between the π-electrons of benzene ring, O and N atoms, and the vacant d-orbitals of iron atoms.

Quantum chemical indices containing E_{HOMO}, E_{LUMO}, ΔE, and Dipole moment (μ) are −6.3104 eV, −1.8768 eV, −4.4336 eV and 2.7648, respectively. It has been reported that excellent inhibition corrosion properties are usually obtained using organic compounds that not only offer electrons to unoccupied orbitals of the metal but also accept free electrons from the metal by using their anti-bond orbitals to form stable chelates [41]. By looking to the Fig. 12, it is understandable that PDQ also could accept the d-orbital electrons of iron by LUMO on the benzene ring and N atoms. Consequently, this electron acceptance could help to form more stable bond between inhibitor molecule and iron surface.

4. Conclusion

Effect of PDQ as an inhibitor of mild steel in 0.1 M HCl solution of was investigated and following results was obtained:

1. PDQ shows inhibition properties in hydrochloric acid by adsorption on metal surface. The beneficial condition among the investigated inhibitors concentrations was 200 ppm with the approximate efficiency of 93%.
2. PDQ acts as an adsorptive inhibitor. It reduces anodic dissolution, retards the hydrogen evolution reaction via blocking the active reaction sites on the metal surface and its adsorption obeys the Langmuir's adsorption isotherm.
3. By increasing the temperature corrosion current density increases, however the rate of its increase is lower at the presence of PDQ.
4. Thermodynamic adsorption parameters such as $\Delta G_{\text{ads}}{}^{\circ}$, $\Delta H_{\text{ads}}{}^{\circ}$ and $\Delta S_{\text{ads}}{}^{\circ}$, show that PDQ is adsorbed by a spontaneous exothermic process and its adsorption is combination of physical and chemical adsorption.
5. Quantum chemical method shows that PDQ molecules can be directly adsorbed at the steel surface on the basis of donor–acceptor interactions between the π-electrons of benzene ring, O and N atoms, and the vacant d-orbitals of iron atoms.

Acknowledgments

Authors would like to appreciate the financial support from Ferdowsi University of Mashhad provision of laboratory facilities during the period that this research was conducted.

References

[1] H.L. Wang, H.B. Fan, J.S. Zheng, Mater. Chem. Phys. 77 (2002) 655.
[2] S.A. Abd El-Maksoud, A.S. Fouda, Mater. Chem. Phys. 93 (2005) 84.
[3] M.A. Migahed, I.F. Nassar, Electrochim. Acta 53 (2008) 2877.

[4] M.A. Migahed, M. Abd-El-Raouf, A.M. Al-Sabagh, H.M. Abd-El-Bary, Electrochim. Acta 50 (2005) 4683.
[5] L. Wang, Corros. Sci. 43 (2001) 2281.
[6] H. Amar, A. Tounsi, A. Makayssi, A. Derja, J. Benzakour, A. Outzourhit, Corros. Sci. 49 (2007) 2936.
[7] J. Cruz, R. Martínez, J. Genesca, E. García-Ochoa, Electroanal. Chem. 566 (2004) 111.
[8] M.A. Khalifa, M. El-Batouti, F. Mahgoub, A. Bakr Aknish, Mater. Corros. 54 (2003) 251.
[9] O. Benali, L. Larabi, M. Traisnel, L. Gengembra, Y. Harek, Appl. Surf. Sci. 253 (2007) 6130.
[10] F. Bentiss, M. Lebrini, M. Lagrenée, Corros. Sci. 47 (2005) 2915.
[11] F. Bentiss, M. Lagrenee, M. Traisnel, B. Mernari, H. Elattari, J. Appl. Electrochem. 29 (1999) 1073.
[12] O. Benali, L. Larabi, Y. Harek, J. Appl. Electrochem. 39 (2009) 769.
[13] F. Bentiss, M. Lagrene'e, M. Traisnel, Corrosion 56 (2000) 733.
[14] E. Naderi, A.H. Jafari, M. Ehteshamzadeh, M.G. Hosseini, Mater. Chem. Phys. 115 (2009) 852.
[15] F. Bentiss, M. Lagrenee, M. Traisnel, J.C. Hornez, Corros. Sci. 41 (1999) 789.
[16] M. Lebrini, M. Traisnel, M. Lagrenee, B. Mernari, F. Bentiss, Corros. Sci. 50 (2008) 473.
[17] M. Lebrini, F. Bentiss, H. Vezin, M. Lagrene'e, Corros. Sci. 48 (2006) 1279.
[18] F. Bentiss, M. Lebrini, H. Vezin, M. Lagrenée, Mater. Chem. Phys. 87 (2004) 18.
[19] M. Outirite, M. Lagrenée, M. Lebrini, M. Traisnel, C. Jama, H. Vezin, F. Bentiss, Electrochim. Acta 55 (2010) 1670.
[20] F. Bentiss, F. Gassam, D. Barbry, L. Gengembre, H. Vezin, M. Lagrene'e, M. Traisnel, Appl. Surf. Sci. 252 (2006) 2684.
[21] M. Bakavoli, A. Shiri, Z. Ebrahimpour, M. Rahimizadeh, Chin. Chem. Lett. 19 (2008) 1403.
[22] ASTM G5-94, Standard Reference Test Method for Making Potentiostatic and Potentiodynamic Anodic Polarization Measurements.
[23] L. Tang, G. Mu, G. Liu, Corros. Sci. 45 (2003) 2251.
[24] J. Aljourani, K. Raeissi, M.A. Golozar, Corros. Sci. 51 (2009) 1836.
[25] A. Popova, M. Christov, A. Vasilev, Corros. Sci. 49 (2007) 3290.
[26] R. Solmaz, G. Kardaş, M. Çulha, B. Yazici, M. Erbil, Electrochim. Acta 53 (2008) 5941.
[27] A. Lgamri, H. Abou El Makarim, A. Guenbour, A. Ben Bachir, L. Aries, S. El Hajjaji, Prog. Org. Coat. 48 (2003) 63.
[28] A. Subrmania, N.T. Kalyana Sundaram, R. Sathiya Priya, K. Saminathan, V.S. Muralidharan, T. Vasudevan, J. Appl. Electrochem. 34 (2004) 693.
[29] Z. Tao, S. Zhang, W. Li, B. Hou, Corros. Sci. 51 (2009) 2588.
[30] S.F. Mertens, C. Xhoffer, B.C. Decooman, E. Temmerman, Corrosion 53 (1997) 381.
[31] H.H. Hassan, Electrochim. Acta 51 (2006) 5966.
[32] E.A. Noor, A.H. Al-Moubaraki, Mater. Chem. Phys. 110 (2008) 145.
[33] G. Avci, Colloid Surf. A 317 (2008) 730.
[34] E. Machnikova, H. Kenton, N. Whitmire, Hackerman, Electrochim. Acta 53 (2008) 6024.
[35] F. Xu, J. Duan, S. Zhang, B. Hou, Mater. Lett. 62 (2008) 4072.
[36] R. Solmaz, G. Kardas, B. Yazici, M. Erbil, Colloid Surf. A 312 (2008) 1.
[37] H. Ashassi-Sorkhabi, B. Shaabani, D. Seifzadeh, Appl. Surf. Sci. 239 (2005) 154.
[38] S.M.A. Hosseini, A. Azimi, Corros. Sci. 51 (2009) 728.
[39] X. Li, S. Deng, H. Fu, G. Mu, Corros. Sci. 51 (2009) 620.
[40] H.L. Wang, H.-B. Fan, J.S. Zheng, Mater. Chem. Phys. 77 (2002) 655.
[41] L. Herrag, B. Hammouti, S. Elkadiri, A. Aouniti, C. Jama, H. Vezin, F. Bentiss, Corros. Sci. 52 (2010) 3042.